Energy bonds as correlators for long-range symmetry-protected topological models and models with long-range topological order

Wing Chi Yu,[1,*] Chen Cheng,[2,4] and P. D. Sacramento[3,4,†]
[1]*Department of Physics, City University of Hong Kong, Hong Kong*
[2]*School of Physical Science and Technology, Lanzhou University, Lanzhou 730000, China*
[3]*CeFEMA, Instituto Superior Técnico, Universidade de Lisboa, Av. Rovisco Pais, 1049-001 Lisboa, Portugal*
[4]*Beijing Computational Science Research Center, Beijing, China*

(Received 25 March 2020; revised manuscript received 15 May 2020; accepted 26 May 2020; published 8 June 2020)

Topological properties are associated with nonlocal entanglement and global properties. On the other hand, in some topological systems, it has been shown that quasilocal operators detect topological transitions. We show in this work that in the case of noninteracting long-range symmetry-protected topological models, energy bonds signal topological transitions. Interestingly, we also find that they display some signatures at the Berezinskii-Kosterlitz-Thouless transition that occurs in a spin chain with first and second neighbor interactions, if we consider the first excited state instead of the ground state of the system. Moreover, we show that the ground-state topological transition in the spin Kitaev model in a honeycomb lattice, which displays topological long-range order, is also detected by the energy bond correlator. Despite the model being interacting, in the ground state it reduces to a noninteracting model. Even for the spin-liquid phase of the two-dimensional Heisenberg model with first and second neighbor interactions, where the system has true long-range entanglement and topological order, the local bonds do signal the topological phase transition.

DOI: 10.1103/PhysRevB.101.245131

I. INTRODUCTION

In condensed matter physics, finding the appropriate parameter that characterizes the long-range correlation in a quantum phase and detects the quantum phase transition is highly nontrivial. Especially for topological systems, in which the phase transition falls beyond the framework of traditional Landau's theory, there is no obvious clue about the order parameter that can be gained from the symmetry of the Hamiltonian. Regarding this, some of the authors have proposed a nonvariational scheme to derive the order parameters systematically in a general model, by analyzing the reduced density matrix spectrum of a model's subsystem [1]. The scheme has been testified in a number of condensed matter systems, such as the Heisenberg model [1] and the fermion Hubbard model [2]. Remarkably, the correlator for the topological phase in topological insulators, such as the Su-Schreiffer-Heeger (SSH) model [3–5] and topological superconductors such as the Kitaev chain [6], were also derived using a modified version of our scheme [7,8]. Comparing to the common approach of using the topological invariants or the entanglement spectrum [9] to study topological phases, the correlators provide us physical insights about the topological phases in real space.

Intriguingly, we observed that the correlators obtained in the SSH and the Kitaev model take a very similar form to the local Hamiltonian of the model, at a specific value of the driving parameter. That is, for $H = \sum_i h_i(\lambda)$, where h_i is the local Hamiltonian and λ is the driving parameter, one can take the correlator as $h_i(\lambda_0)$, where λ_0 is a specific value of the driving parameter. We found that the first derivative of the ground-state expectation value of such a correlator is able to capture the topological transition in the SSH-Kitaev model [8]. This raises the question whether such a simple local or quasilocal bond correlator can be used as an indicator of the transition in topological models with long-range couplings in the Hamiltonian or long-range topological orders in the ground state. To answer this question is the primary motivation of the present work. The computation of topological invariants or entanglement spectrum can be complicated and time-consuming since, for the former case, one has to impose twisted boundary conditions if the Berry phase is considered, and for the latter case the half block reduced density matrix has to be calculated. In contrast, the expectation value of the local bond correlator is straightforward to be computed. Therefore, if it works, the bond correlator will be a convenient tool to study the topological phase transitions, due to its simplicity.

In the following, we consider long-range models with symmetry-protected topological phases and models with long-range topological orders. In particular, the bond correlators for the Kitaev chain with long-range hopping and interactions [10], the spin Kitaev model on a honeycomb lattice [11], and the one-dimensional (1D) and two-dimensional (2D) J1-J2 spin-half Heisenberg models [12–14] are investigated. We find that the bond correlators, or its first derivative, are able to

*wingcyu@cityu.edu.hk
†pdss@cefema.tecnico.ulisboa.pt

detect the transitions in the symmetry-protected topological models. Moreover, they are also able to detect the topological transition of the spin two-dimensional Kitaev model on the honeycomb lattice. Even though the model has in general topological order, it reduces to a noninteracting model in the ground state. Interestingly, the bond correlators also show some nontrivial features at a Berenzinskii-Kosterlitz-Thouless (BKT) transition, considering the average value of the energy bond in the first excited state of the interacting spin-1/2 chain with first and second neighbor interactions. Even for the 2D J1-J2 model, in which the spin-liquid phase exhibits a true topological long-range order, the quasilocal bond correlators also show signatures around the topological phase transition.

II. KITAEV CHAIN WITH LONG-RANGE HOPPING AND INTERACTIONS

The Hamiltonian of the model reads [10]

$$H=\sum_{j=1}^{N}\left[-t\sum_{l=1}^{N-1}\frac{1}{r_{l,\xi}}c_j^{\dagger}c_{j+l}+d\sum_{l=1}^{N-1}\frac{1}{R_{l,\alpha}}c_jc_{j+l}-\frac{\mu}{2}\left(c_j^{\dagger}c_j-\frac{1}{2}\right)+\text{H.c.}\right], \tag{1}$$

where c_j ($c_j^{\dagger}$) are spinless fermionic annihilation (creation) operators and μ is the chemical potential. N is the number of sites in the chain and is taken as 200 in our simulation, unless otherwise specified. The hopping and the paring amplitude are given by t and d, respectively. Without loss of generality, we consider $t=d=0.5$. The parameters $r_{l,\xi}$ and $R_{l,\alpha}$ are generic functions of the distance l; ξ and α, respectively, characterize the long-range nature of the hopping and pairing terms. We can write the Hamiltonian in the form of $H=\sum_j h_j(\xi,\alpha,\mu)$. When only the nearest-neighbor hoppings and pairings are considered, the model reduces to the usual Kitaev chain and the system is topological for $-1\leqslant\mu\leqslant 1$ [6].

First, let us consider the Hamiltonian in Eq. (1) with nearest-neighbor pairing and exponentially decaying hopping, i.e., $R_{1,\alpha}=1$, $R_{l>1,\alpha}=\infty$, and $r_{l,\xi}=\exp[(l-1)/\xi]$. An augmented topological phase was observed with an increasing ξ in the model [10]. If we fix $\xi=1$ and change the chemical potential μ from -3 to 2, the system goes from a trivial ($-3\leqslant\mu\lesssim-1.5$) to topological ($-1.5<\mu\lesssim 0.8$) to trivial phase ($0.8<\mu\leqslant 2$). Figure 1 shows the energy bond correlators $C_{\mu_0}=\langle h_j(\mu_0)\rangle$ calculated by taking $\mu_0=-3,0,1.5$, respectively. Note that the correlator involves an extensive number of terms. We consider a site near the middle of the chain and a number of neighbors that has a length of the order of half the chain length. There are small kinks in the correlator that appear at the topological phase transition points located at $\mu\approx-1.5$ and 0.8. If we calculate the first derivative of the correlators with respect to μ, we can see that the critical points are detected by the singular peaks in the absolute value of the first derivative of the correlators. Moreover, the absolute value of the first derivative of the correlator has the vanishing amplitude in the phase in which μ_0 is taken from.

In Fig. 2, we fix $\mu=-3$ and change the penetration length $0.5<\xi<5$. The system goes from the trivial to the topological phase and the transition takes place at $\xi\approx 2.5$ [10].

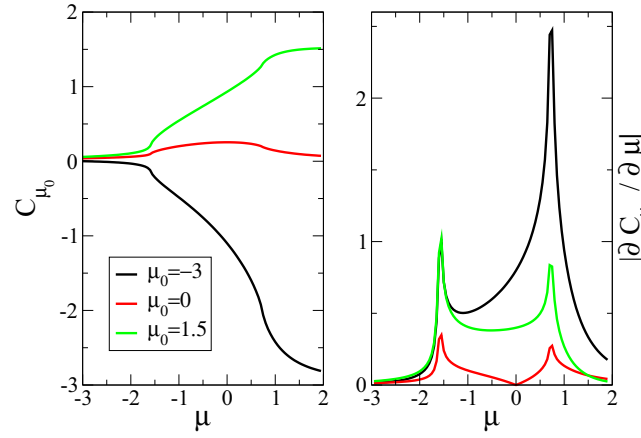

FIG. 1. The bond correlators C_{μ_0} with $\mu_0=-3,0,1.5$, respectively, and the absolute value of the derivatives of the long-range Kitaev chain. The pairing is between nearest neighbors and the hopping decays exponentially. Here we fix $\xi=1$ and change the chemical potential μ.

The energy bond correlators $C_{\xi_0}=\langle h_j(\xi_0)\rangle$ are calculated by taking $\xi_0=0.5,1.5,3,4$. Again, the topological transition is signaled by the dominating peaks in the first derivative of the correlators.

Next, we consider only the nearest-neighbor hopping but a power-law decay in the pairing terms with an exponent α, i.e., $r_{1,\xi}=1$, $r_{l>1,\xi}=\infty$, and $R_{\alpha,l}=l^{\alpha}$. Interestingly, three topological sectors are found in this case [10]: (1) a Majorana sector for $\alpha>3/2$; (2) a massive Dirac sector for $\alpha<1$; and (3) a crossover sector for $\alpha\in(1,3/2)$.

Consider a cut along α with fix $\mu=0$. Figure 3 shows the result of the bond correlators $C_{\alpha_0}=\langle h_j(\alpha_0)\rangle$ taken at $\alpha_0=0.2,0.5,1.25,2$ and the respective absolute value of the first derivatives. The first derivative shows a blob in the vicinity of the crossover region but there is no clear signal of the transition at $\alpha=1$ from the massive to massless Majorana sector. In Fig. 4, we plot the second derivative of the C_{α_0}

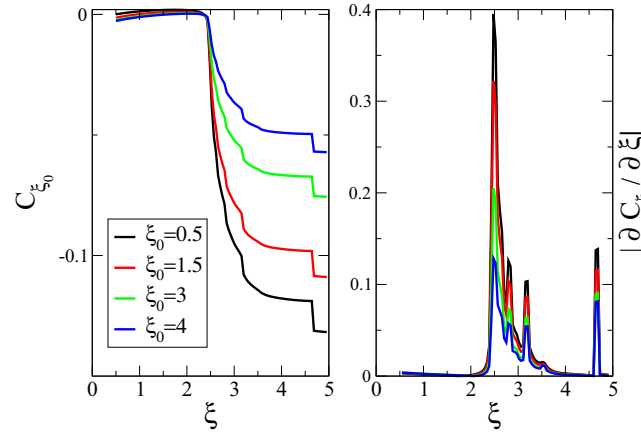

FIG. 2. Correlators C_{ξ_0} and the absolute value of the derivatives of the correlators of the long-range Kitaev model. The pairing is between nearest neighbors and the hopping decays exponentially. Here we fix $\mu=-3$ and change the penetration length ξ.

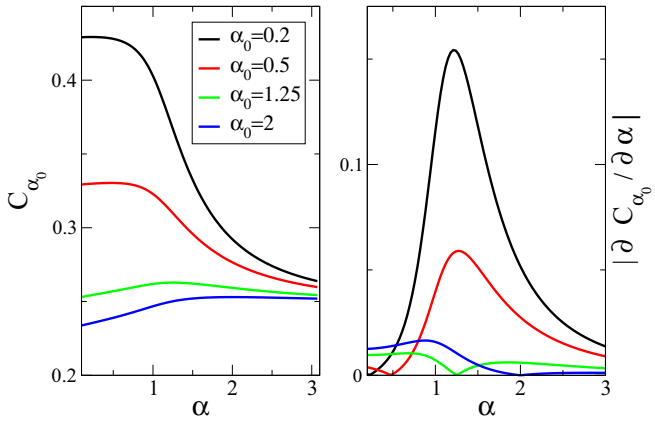

FIG. 3. Correlators C_{α_0} and the absolute value of the derivatives of the correlators in the long-range Kitaev model. The hopping is between nearest neighbors and the pairing decays as a power law with exponent α. Here we fix $\mu = 0$ and change the exponent α.

as a function of α. Physically, the second derivatives of the energy can be regarded as the susceptibilities, and have been conventionally used as an indicator of a continuous phase transition. Intriguingly, from Fig. 4, the second derivatives of the bond energy correlators are able to signal the transitions to the Majorana and the Dirac sectors in the system as reflected by two clear peaks around $\alpha = 1$ and $\alpha = 1.5$. We have also checked that the first derivatives of the correlators detect the transition from the topological to a trivial phase, considering a cut as a function of the chemical potential μ for $\alpha = 2$.

In Fig. 5 we consider the same parameters as in Fig. 1, except that we take $\xi = 2$. That is, we consider the model with exponentially decaying hopping and pairing only between nearest neighbors. The special points are taken as before as $\mu_0 = -3, 0, 1.5$. However, here we take the correlator $\bar{C}_{\mu_0}$ not as a sum of terms from the middle point of the chain until the end (and therefore a number of terms that is half the system size) but we take only the chemical potential term at the middle point of the chain. So, a completely local term. Notice that the term in the Hamiltonian comes multiplied by

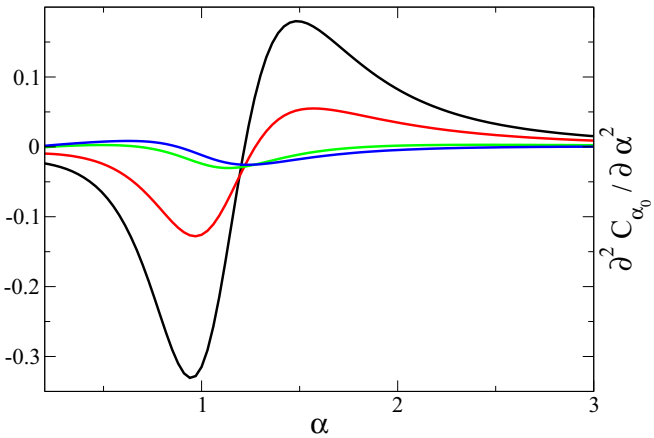

FIG. 4. Second derivatives of the correlators C_{α_0} in Fig. 3. The parameters and the color scheme of the curves are the same as that in Fig. 3.

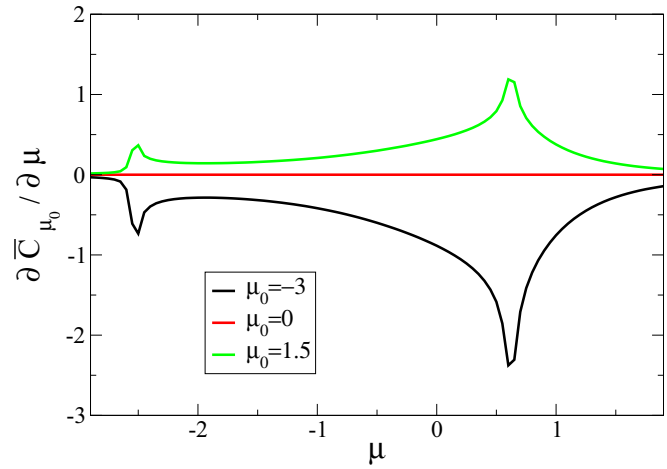

FIG. 5. Derivative of the chemical potential term of the Hamiltonian of the long-range Kitaev model. We use the same parameters as in Fig. 1 except that we take $\xi = 2$. Note that the correlator $\bar{C}_{\mu_0}$ considered here is completely local. The results are for the middle point of the chain.

the chemical potential at a special point and so the curve with $\mu_0 = 0$ vanishes. The other two values give surprising results since the correlators and the derivatives are very similar to the full expression for the bond energy, h_i, that includes the chemical potential term and the hoppings and pairings over an extensive number of neighbors. This shows that the dominant contribution is due to the term that is associated with the variable that defines the cut. Since, in this case, the cut is obtained changing the chemical potential, the result is mainly due to the term associated with the chemical potential. In this case this is a local contribution. The information on the long-range nature of the model is therefore to be completely contained in the states, as the approach using the reduced density matrix might suggest, and the average of the operator just reveals the change of the states as one crosses the transition point. So if a transition is obtained changing a given parameter, it is enough to consider the operator associated with this change and, at least its derivative, may be used to detect the phase transitions.

III. KITAEV MODEL ON A HONEYCOMB LATTICE

In this section, we investigate the energy bond correlator in the interacting 2D Kitaev model. The Hamiltonian reads [11]

$$H = -J_x \sum_{x\text{ bond}} \sigma_j^x \sigma_k^x - J_y \sum_{y\text{ bond}} \sigma_j^y \sigma_k^y - J_z \sum_{z\text{ bond}} \sigma_j^z \sigma_k^z, \quad (2)$$

where σ_κ with $\kappa = x, y, z$ are the Pauli matrices, and J_x, J_y, J_z are the spin-spin interaction strength along the x, y, z bonds, respectively. Figure 6(a) shows a schematic illustration of the model. This is one of the very few interacting models in two dimensions that the ground state can be solved analytically by mapping the model to a Majorana fermion model [11] or by using the Jordan-Wigner transformation in 2D [15]. The Hamiltonian commutes with the plaquette operators $W_p = \sigma_1^x \sigma_2^y \sigma_3^z \sigma_4^x \sigma_5^y \sigma_6^z$ which have eigenvalues of $w_p = \pm 1$. The ground state of the system lies in the vortex-free subspace in which all the plaquette operators have eigenvalues of $+1$.

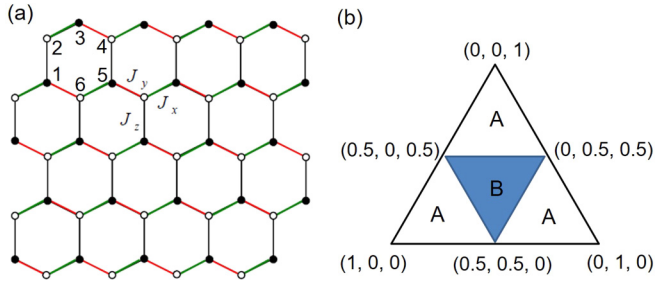

FIG. 6. (a) A schematic diagram of the Kitaev model on the honeycomb lattice. (b) A schematic phase diagram of the 2D Kitaev model on the $J_x + J_y + J_z = 1$ plane. The A phase is gapped and topological while the B phase is gapless and topologically trivial. The values inside the brackets indicate the coordinates (J_x, J_y, J_z) of the corresponding point.

An excitation is to create vortices ($w_p = -1$) as described by non-Abelian anyons.

For $|J_z| \leqslant |J_x| + |J_y|$, $|J_x| \leqslant |J_y| + |J_z|$, and $|J_y| \leqslant |J_z| + |J_x|$, the system is in the gapless phase, which is topological and the excitation satisfies the non-Abelian anyons. Otherwise, the system is in a gapped trivial phase [11,15]. A schematic phase diagram on the $J_x + J_y + J_z = 1$ plane is shown in Fig. 6(b). The trivial and topological phases are denoted as the A and B phase, respectively. In the following, we consider J_z as the driving parameter along $J_x = J_y$ on the plane. The system goes from the gapless topological B phase to the gapped trivial A phase. A topological quantum phase transition occurs at $J_z = 0.5$.

Consider the correlators defined by the ground-state expectation values of the energy bond operator taken at two specific points of the phase diagram, i.e., $(J_{x0}, J_{y0}, J_{z0}) = (0, 0, 1)$ and (0.5,0.5,0), respectively. Explicitly, the correlators can be expressed as

$$C_z = \langle \sigma^z_{\mathbf{r}} \sigma^z_{\mathbf{r}+\mathbf{z}} \rangle, \tag{3}$$

$$C_{xy} = \langle 0.5\sigma^x_{\mathbf{r}} \sigma^x_{\mathbf{r}+\mathbf{x}} + 0.5\sigma^y_{\mathbf{r}} \sigma^y_{\mathbf{r}+\mathbf{y}} \rangle, \tag{4}$$

where $\mathbf{r}$ and $\mathbf{r} + \kappa (\kappa = \mathbf{x}, \mathbf{y}, \mathbf{z})$ is the position vector to the middle site and that of its nearest-neighbor site along the corresponding direction, respectively. Using the Hellmann-Feynman theorem, we have

$$\langle \sigma^x_{\mathbf{r}} \sigma^x_{\mathbf{r}+\mathbf{x}} \rangle = \frac{1}{L^2} \sum_{q_x, q_y} \left(\frac{\epsilon_{\mathbf{q}} \cos q_x + \Delta_{\mathbf{q}} \sin q_x}{\sqrt{\epsilon^2_{\mathbf{q}} + \Delta^2_{\mathbf{q}}}} \right),$$

$$\langle \sigma^y_{\mathbf{r}} \sigma^y_{\mathbf{r}+\mathbf{y}} \rangle = \frac{1}{L^2} \sum_{q_x, q_y} \left(\frac{\epsilon_{\mathbf{q}} \cos q_y + \Delta_{\mathbf{q}} \sin q_y}{\sqrt{\epsilon^2_{\mathbf{q}} + \Delta^2_{\mathbf{q}}}} \right),$$

$$\langle \sigma^z_{\mathbf{r}} \sigma^z_{\mathbf{r}+\mathbf{z}} \rangle = \frac{1}{L^2} \sum_{q_x, q_y} \left(\frac{\epsilon_{\mathbf{q}}}{\sqrt{\epsilon^2_{\mathbf{q}} + \Delta^2_{\mathbf{q}}}} \right), \tag{5}$$

where

$$\epsilon_{\mathbf{q}} = J_z - J_x \cos q_x - J_y \cos q_y, \tag{6}$$

$$\Delta_{\mathbf{q}} = J_x \sin q_x + J_y \sin q_y. \tag{7}$$

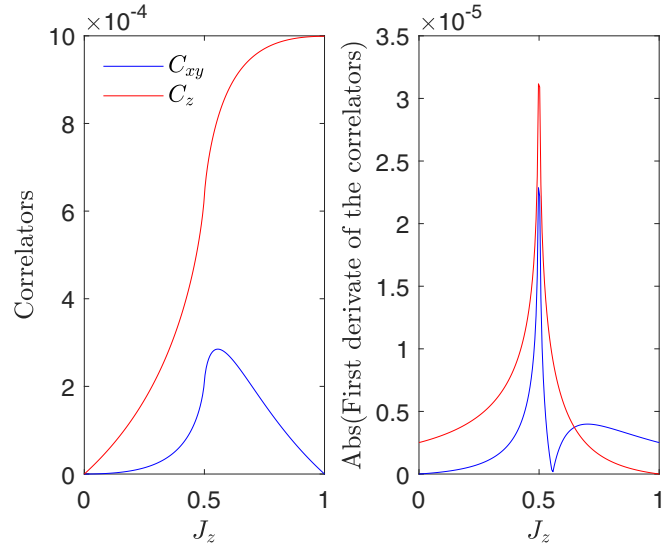

FIG. 7. The bond correlators and the absolute value of its first derivatives in the 2D honeycomb lattice Kitaev model as a function of J_z.

The system size along one direction is $L = L_x = L_y$ and is taken to be 1001 in our simulation. The momentum wave vector $q_{x(y)} = 2m\pi/L$ with $m = -(L-1)/2 \cdots (L-1)/2$.

The result of the bond correlators and the absolute value of its first derivative are shown in Fig. 7. The first derivative of the correlators shows singular peaks at the model's topological quantum phase transition point, and thus can be used to signal the transition. Furthermore, the absolute value of the first derivative of the correlator goes to zero in the corresponding phase from which (J_{x0}, J_{y0}, J_{z0}) are chosen.

IV. ONE-DIMENSIONAL J_1-J_2 MODEL

Another model we have considered is the 1D Heisenberg model with first and second neighbor interactions, also called the J_1-J_2 model. The Hamiltonian of the model is given by

$$H = J_1 \sum_{\langle i,j \rangle} \mathbf{S}_i \cdot \mathbf{S}_j + J_2 \sum_{\langle\langle i,j \rangle\rangle} \mathbf{S}_i \cdot \mathbf{S}_j, \tag{8}$$

where $\mathbf{S}_j = (S^x_j, S^y_j, S^z_j)$ is the spin-1/2 operator, $\langle i, j \rangle$ and $\langle\langle i, j \rangle\rangle$ denote the nearest and the next-nearest neighbors, respectively. The system undergoes a BKT quantum phase transition at $J_2/J_1 = 0.24$ [16,17]. For $J_2/J_1 < 0.24$, the system has a gapless Heisenberg-like ground state with power-law decay spin-spin correlations. For $J_2/J_1 > 0.24$, the ground state is doubly degenerate and the spectrum has a spin gap with power-law decay bond-bond correlations. At the Majumdar Ghosh point where $J_2/J_1 = 0.5$, the ground state is a product state of singlet pairs and is twofold degenerated for any system size [18–20]. In the gapped phase the antiferromagnetic correlations between second neighbors become dominant.

Let us define the correlators by considering the specific points where $(J_{1,0}, J_{2,0}) = (1, 0)$ and (0,1), respectively. We have

$$C_1 = \langle \mathbf{S}_j \cdot \mathbf{S}_{j+1} \rangle, \quad C_2 = \langle \mathbf{S}_j \cdot \mathbf{S}_{j+2} \rangle. \tag{9}$$

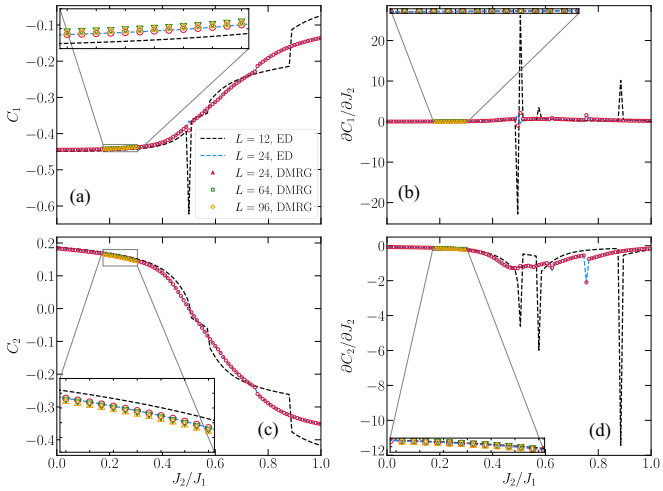

FIG. 8. (a) and (b) show the bond correlator C_1 and its first derivative, respectively, for various system sizes. (c) and (d) show the bond correlator C_2 and its first derivative, respectively. Insets show a zoom-in of the curves around the BKT transition point.

We first consider the average taken with respect to the ground state of the system and the results are shown in Fig. 8. The simulation is performed with numerical Lanczos exact diagonalization (ED) for a system size $L = 12$ and $L = 24$, and with density-matrix renormalization group (DMRG) [21,22] for $L = 24, 64, 96$. We dynamically use up to 2000 DMRG many-body states so that the truncation error is smaller than 10^{-10} [23]. Periodic boundary condition is adopted for both ED and DMRG calculations. For a small system, discontinuities are observed around the Majumdar-Ghosh point. At this special point, the ground state is twofold degenerated under the periodic boundary condition and a numerically obtained ground state will give a random value in the observables. Kinks in the correlators and thus peaks or dips in the first derivatives of the correlators are also observed at some other values of J_2/J_1; for example, around 0.9 for $L = 12$. They seem to be suppressed for a larger system $L = 24$. We may attribute those discontinuities to the level crossing between the ground state and the lowest excited state in the energy spectrum as shown in the energy spectrum in Fig. 9. For the BKT transition point at $J_2/J_1 = 0.24$, no signature of the phase transition is found in the correlators.

It is not surprising that the energy bond correlators calculated from the ground state do not detect the BKT transition at $J_2/J_1 = 0.24$. As we can see from the energy spectrum in Fig. 9, the BKT transition arises from the level crossing in the first excited states of the $S^z_{\text{total}} = 0$ sector. Instead of the ground state, we can consider the bond operators average with respect to the first excited state. Figure 10 shows the bond correlator $C_1 + C_2$, which corresponds to the local Hamiltonian at $J_{2,0}/J_{1,0} = 1$, calculated using the first excited state as a function of J_2/J_1. Discontinuities are observed at the BKT transition point and some other values of J_2/J_1. In the figure, we compared the bond correlator of different system sizes. The discontinuities away from $J_2/J_1 = 0.24$ seem to be smeared out while the one at the BKT transition

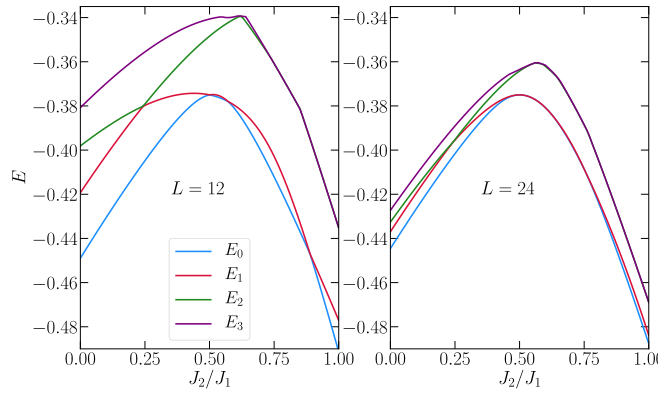

FIG. 9. Energy spectrum as a function of J_2/J_1 for the 1D J_1-J_2 model in the $S^z_{\text{total}} = 0$ sector obtained from ED. Only the first four eigenenergies are shown.

remains, but becomes less pronounced, as the system size increases.

In the $S^z_{\text{total}} = 0$ sector, the first excited state for $J_2/J_1 < 0.24$ has a total spin $S = 1$. However, for $J_2/J_1 > 0.24$, the first excited state has a total spin of $S = 0$. Alternatively, one can determine the phase transition point by directly checking the total spin of the first excited states in the $S^z_{\text{total}} = 0$ sector. For examples, one can consider the bond correlator

$$C_S(r) = \langle S^+_j S^-_{j+r} - S^z_j S^z_{j+r} \rangle, \tag{10}$$

where $S^\pm_j = S^x_j \pm iS^y_j$. Figure 11 shows the correlator calculated with respect to the ground state and the first excited state. No signature for the transition is observed in the ground-state average. However, if we calculate C_S with respect to the first excited state, it shows a clear discontinuity at the BKT transition point $J_2/J_1 = 0.24$.

V. TWO-DIMENSIONAL J_1-J_2 MODEL

We considered the J_1-J_2 model described by the Hamiltonian in Eq. (8) on a square lattice. The model was first introduced to describe the breakdown of Néel order in cuprate superconductors [12–14] and has been extensively studied in the past several decades (see, for examples, Refs. [24–29]).

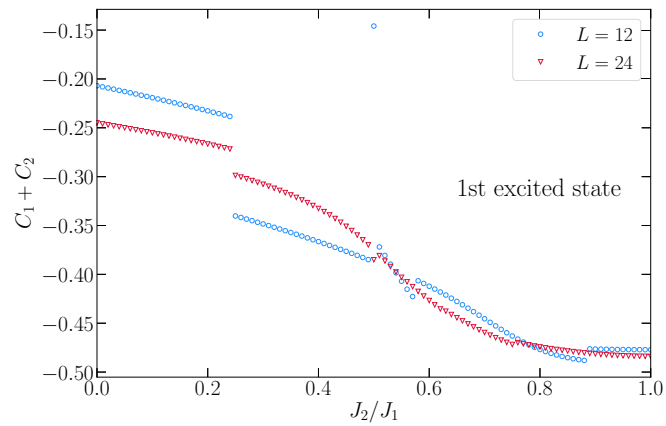

FIG. 10. The correlator $C_1 + C_2$ calculated with respect to the first excited state in the 1D J_1-J_2 model.

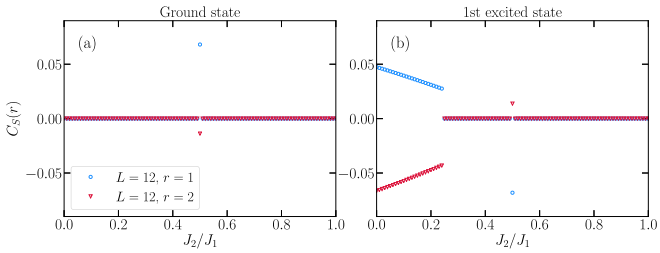

FIG. 11. The correlator C_S in Eq. (10) as a function of J_2/J_1 in the 1D J_1-J_2 model calculated with respect to the ground state (left) and the first excited state (right).

It is generally believed that the ground-state phase diagram has a Néel antiferromagnetic (AFM) order in the small J_2/J_1 region, and a stripe AFM in the large J_2/J_1 region. In between the two phases, there is a spin-liquid phase in the region of $0.4 \lesssim J_2/J_1 \lesssim 0.6$. However, we shall point out that the nature of this intermediate phase is still under debate but it has been determined that there is a finite topological entanglement entropy, and therefore, topological order [26].

We tested our scheme of detecting the phase transition in this model. Enlightened by the 1D case, we compute both the ground state and the first excited state, by using DMRG method. As in most literature, the cylinder geometry is adopted, with open and periodic boundaries in the x and y direction, respectively. We dynamically use up to 4000 DMRG many-body states, and, in most cases, the truncation error is smaller than 10^{-7}. The bond correlators on the 2D cylinder can be defined as

$$C_1^x = \langle \mathbf{S}_{x_0,y_0} \cdot \mathbf{S}_{x_0+1,y_0} \rangle, \quad C_1^y = \langle \mathbf{S}_{x_0,y_0} \cdot \mathbf{S}_{x_0,y_0+1} \rangle,$$
$$C_2 = \langle \mathbf{S}_{x_0,y_0} \cdot \mathbf{S}_{x_0+1,y_0+1} \rangle, \tag{11}$$

where $(x_0, y_0) = (L_x/2, L_y/2)$ is the center site of the lattice. Figure 12 shows the result of the bond correlators C_1^x, C_1^y,

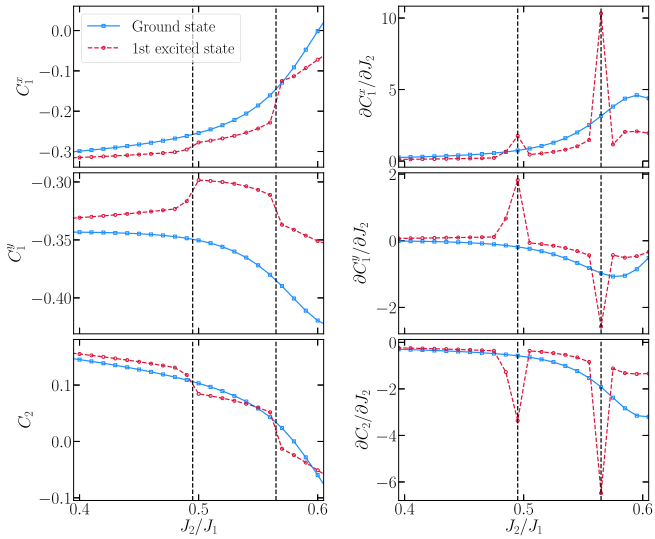

FIG. 12. The bond correlators (left panel) and the first derivatives (right panel) as a function of J_2/J_1 for the J_1-J_2 model on a square lattice. Here $L_x = 12$ and $L_y = 6$.

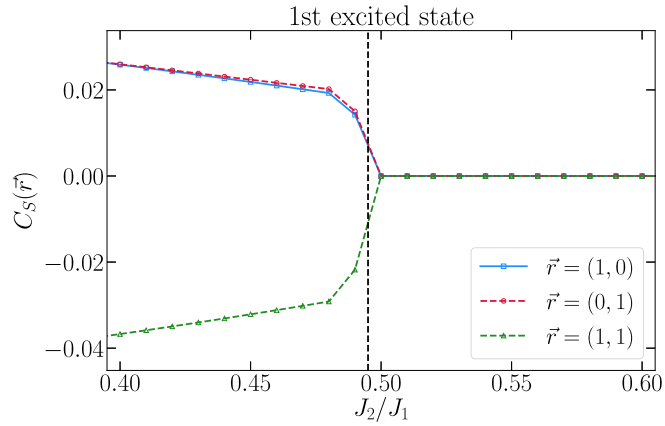

FIG. 13. The correlator C_S in Eq. (10) as a function of J_2/J_1 for the J_1-J_2 model on a square lattice. Here $L_x = 12$ and $L_y = 6$.

and C_2 and their first derivatives. For the ground state, all the presented quantities behave smoothly in the range of J_2/J_1 considered and no signatures of the transition were found. On the other hand, for the first excited state, bond correlators do show some anomalies. Similar to Eq. (10) in the 1D case, we also consider the local bond correlator to check whether a state has zero total spin. The result of the first excited state is shown in Fig. 13. Here, only one anomaly between $J_2/J_1 = 0.49$ and 0.50 can be observed. By carefully comparing our results and the results in Ref. [29], this anomaly corresponds to the transition between the spin-liquid and the stripe AFM phase.

The ground state of the 2D J_1-J_2 model is still under controversy. From our current results we cannot conclude that the bond correlators have successfully detected all quantum phase transitions in this model. In addition, the second anomaly in Fig. 12 may correspond to higher excited level crossings, or may be just a finite-size effect. A clear answer to these uncertainties, which is not our aim in this work, requires proper finite size with results from larger lattices and heavy numerics.

VI. CONCLUSION

We examined the capability of the bond correlators in detecting topological phase transitions in various models which possess symmetry-protected topological phases or long-range topological orders. We first considered the Kitaev chain with long-range hopping and interactions. The topological phase transitions in the system were detected by the peaks or dips in the first derivative of the bond correlators with respect to the driving parameters. The rate of change in the bond correlators selected from the corresponding phase was also found to be minimum. We also considered the interacting spin Kitaev model on a honeycomb lattice. Interestingly, similar observations about the bond correlators were obtained. Moreover, for the BKT transition in the 1D J_1-J_2 model, nontrivial features in the bond correlators were also found by taking the average value with respect to the first excited state. For the 2D J_1-J_2 model on the square lattice, the local bond correlators show some anomalies as well. Although we cannot conclude that these anomalies correspond to quantum critical points, the local bonds show the potential to detect a phase

with true topological long-range order and finite topological entanglement entropy.

It is generally believed that a measurement of the system's global properties is required to characterize a topological phase transition. However, in this work, we showed that local bond operators can be potential candidates of signaling the topological transitions in the models being studied. In fact, there also exist studies suggesting that local operators can be used to detect the topological transition. For example, by measuring the charge imbalance, the transition of the Haldane phase can be detected [30,31]. Another example is the presence of Majorana states in topological superconductors that can be detected by local Majorana polarization [32,33]. For future works, it will be useful to understand the physical reason behind why the local bond correlators work or when they will fail. This could help us further grasp the topological nature of the transition from the bond energy perspectives.

ACKNOWLEDGMENTS

We thank H.-Q. Lin and Y. Li for helpful discussions. W.C.Y. thanks the Beijing Computational Science Research Center for the hospitality during which part of the work was done. This research is financially supported by City University of Hong Kong through Grant No. 9610438 and partially by Fundação para a Ciência e a Tecnologia (Portugal) through Grants No. UID/CTM/04540/2013 and No. UID/CTM/04540/2019. The computations were partially performed in the Tianhe-2JK at the Beijing Computational Science Research Center.

[1] S. J. Gu, W. C. Yu, and H. Q. Lin, Ann. Phys. (NY) **336**, 118 (2013).
[2] W. C. Yu, S. J. Gu, and H. Q. Lin, Eur. Phys. J. B **89**, 212 (2016).
[3] W. P. Su, J. R. Schrieffer, and A. J. Heeger, Phys. Rev. Lett. **42**, 1698 (1979).
[4] W. P. Su, J. R. Schrieffer, and A. J. Heeger, Phys. Rev. B **22**, 2099 (1980).
[5] A. J. Heeger, S. Kivelson, J. R. Schrieffer, and W. P. Su, Rev. Mod. Phys. **60**, 781 (1988).
[6] A. Y. Kitaev, Sov. Phys. Usp. **44**, 131 (2001).
[7] W. C. Yu, Y. C. Li, P. D. Sacramento, and H.-Q. Lin, Phys. Rev. B **94**, 245123 (2016).
[8] W. C. Yu, P. D. Sacramento, Y. C. Li, D. G. Angelakis, and H. Q. Lin, Phys. Rev. B **99**, 115113 (2019).
[9] H. Li and F. D. M. Haldane, Phys. Rev. Lett. **101**, 010504 (2008).
[10] O. Viyuela, D. Vodola, G. Pupillo, and M. A. Martin-Delgado, Phys. Rev. B **94**, 125121 (2016).
[11] A. Kitaev, Ann. Phys. (NY) **321**, 2 (2006).
[12] M. Inui, S. Doniach, and M. Gabay, Phys. Rev. B **38**, 6631 (1988).
[13] P. Chandra and B. Doucot, Phys. Rev. B **38**, 9335 (1988).
[14] E. Dagotto and A. Moreo, Phys. Rev. Lett. **63**, 2148 (1989).
[15] H. D. Chen and Z. Nussinov, J. Phys. A: Math. Theor. **41**, 075001 (2008).
[16] K. Okamoto and K. Nomura, Phys. Lett. A **169**, 433 (1992).
[17] G. Castilla, S. Chakravarty, and V. J. Emery, Phys. Rev. Lett. **75**, 1823 (1995).
[18] C. K. Majumdar and D. K. Ghosh, J. Math. Phys. **10**, 1388 (1969).
[19] C. K. Majumdar and D. K. Ghosh, J. Math. Phys. **10**, 1399 (1969).
[20] C. K. Majumdar, J. Phys. C: Solid State Phys. **3**, 911 (1970).
[21] S. R. White, Phys. Rev. Lett. **69**, 2863 (1992).
[22] S. R. White, Phys. Rev. B **48**, 10345 (1993).
[23] Ö. Legeza, J. Röder, and B. A. Hess, Phys. Rev. B **67**, 125114 (2003).
[24] R. R. P. Singh, Z. Weihong, C. J. Hamer, and J. Oitmaa, Phys. Rev. B **60**, 7278 (1999).
[25] L. Capriotti and S. Sorella, Phys. Rev. Lett. **84**, 3173 (2000).
[26] H. C. Jiang, H. Yao, and L. Balents, Phys. Rev. B **86**, 024424 (2012).
[27] W. J. Hu, F. Becca, A. Parola, and S. Sorella, Phys. Rev. B **88**, 060402(R) (2013).
[28] S. S. Gong, W. Zhu, D. N. Sheng, O. I. Motrunich, and M. P. A. Fisher, Phys. Rev. Lett. **113**, 027201 (2014).
[29] L. Wang and A. W. Sandvik, Phys. Rev. Lett. **121**, 107202 (2018).
[30] F. D. M. Haldane, Phys. Rev. Lett. **61**, 2015 (1988).
[31] B. Grémaud and G. G. Batrouni, Phys. Rev. B **95**, 165131 (2017).
[32] C. Dutreix, M. Guigou, D. Chevallier, and C. Bena, Eur. Phys. J. B **87**, 296 (2014).
[33] D. Sticlet, C. Bena, and P. Simon, Phys. Rev. Lett. **108**, 096802 (2012).